

Comparison of Gediminas Hill slopes behaviour under environmental and fireworks conditions

Šarūnas Skuodis*, Mykolas Daugevičius, Neringa Dirgėlienė, Mindaugas Zakarka

Skuodis, Š., Daugevičius, M., Dirgėlienė, N., Zakarka, M. 2026. Comparison of Gediminas Hill slopes behaviour under environmental and fireworks conditions. *Baltica* 39 (1), 103–113. Vilnius. ISSN 1648-858X.

Manuscript submitted 15 January 2026 / Accepted 28 April 2026 / Available online 20 May 2026

© Baltica 2026

Abstract. This study presents the results of three-dimensional finite element modelling of Gediminas Hill in Vilnius, incorporating existing buildings and the remains of the Upper and Lower Castles. The main objective is to assess slope stability using the strength reduction method and to identify potential critical failure scenarios considering the interaction between soil and structural elements. Both static and dynamic loading conditions are analysed. Static loading includes the self-weight of soil layers, technogenic deposits, structural elements, and infrastructure, while dynamic effects are represented by fireworks-induced impact loads. The comparison of analyses reveals differences in displacement development and failure mechanisms. Strength reduction results highlight the zones of concentrated deformation within the technogenic layer, which are further evaluated in relation to the effects of dynamic loading.

Keywords: slope stability; dynamic loading; fireworks-induced vibrations; 3D finite element analysis

✉ *Šarūnas Skuodis (sarunas.skuodis@vilniustech.lt),  <https://orcid.org/0000-0001-9467-7255>;
Mykolas Daugevičius (mykolas.daugevicius@vilniustech.lt);
Neringa Dirgėlienė (neringa.dirgeliene@vilniustech.lt),  <https://orcid.org/0000-0002-3628-9286>;
Mindaugas Zakarka (mindaugas.zakarka@vilniustech.lt),  <https://orcid.org/0000-0001-7154-1267>
Department of Reinforced Concrete Structures and Geotechnics, Vilnius Gediminas Technical University, Vilnius, Lithuania

*Corresponding author

INTRODUCTION

Lithuania is classified as a low seismic hazard zone in Europe. The country lies in the stable East European Craton, meaning earthquakes are rare and usually of low magnitude. However, hazard maps still assign Lithuania to zones of low but non-zero seismic risk, mainly due to regional tectonic activity in the Baltic and nearby Kaliningrad area. Earthquake frequency is very low: only a few dozen events have been recorded since the 17th century, most below magnitude 5 (Lazauskienė *et al.* 2012). The strongest nearby event was the 2004 Kaliningrad earthquake (M 5.0–5.2), which was felt across Lithuania and prompted reassessment of seismic risk.

According to the European Seismic Hazard Map, Lithuania is in the lowest hazard category (see Fig. 1),

with expected peak ground acceleration (PGA) values typically < 0.04 g (less than 4% of gravity) (Seismic Hazard Map 2025). The Global Seismic Hazard Map (Pagani *et al.* 2018) confirms Lithuania's classification as a low hazard territory, though not completely risk free (Vilnius city is assigned to 10% poe in 50 years with PGA equal to 0.00813134 g). Heritage sites (like Gediminas Hill) and industrial facilities mostly suffer from possible vibrations and rare seismic events, though in some cases it is also necessary to evaluate fireworks loads (for Gediminas Hill, this type loads can appear more often than earthquake loads).

Gediminas Hill in Vilnius is a historic landmark often associated with fireworks displays during national celebrations. Its exploitation is technically regulated due to slope instability and dynamic loading from events, visitors, and infrastructure like the

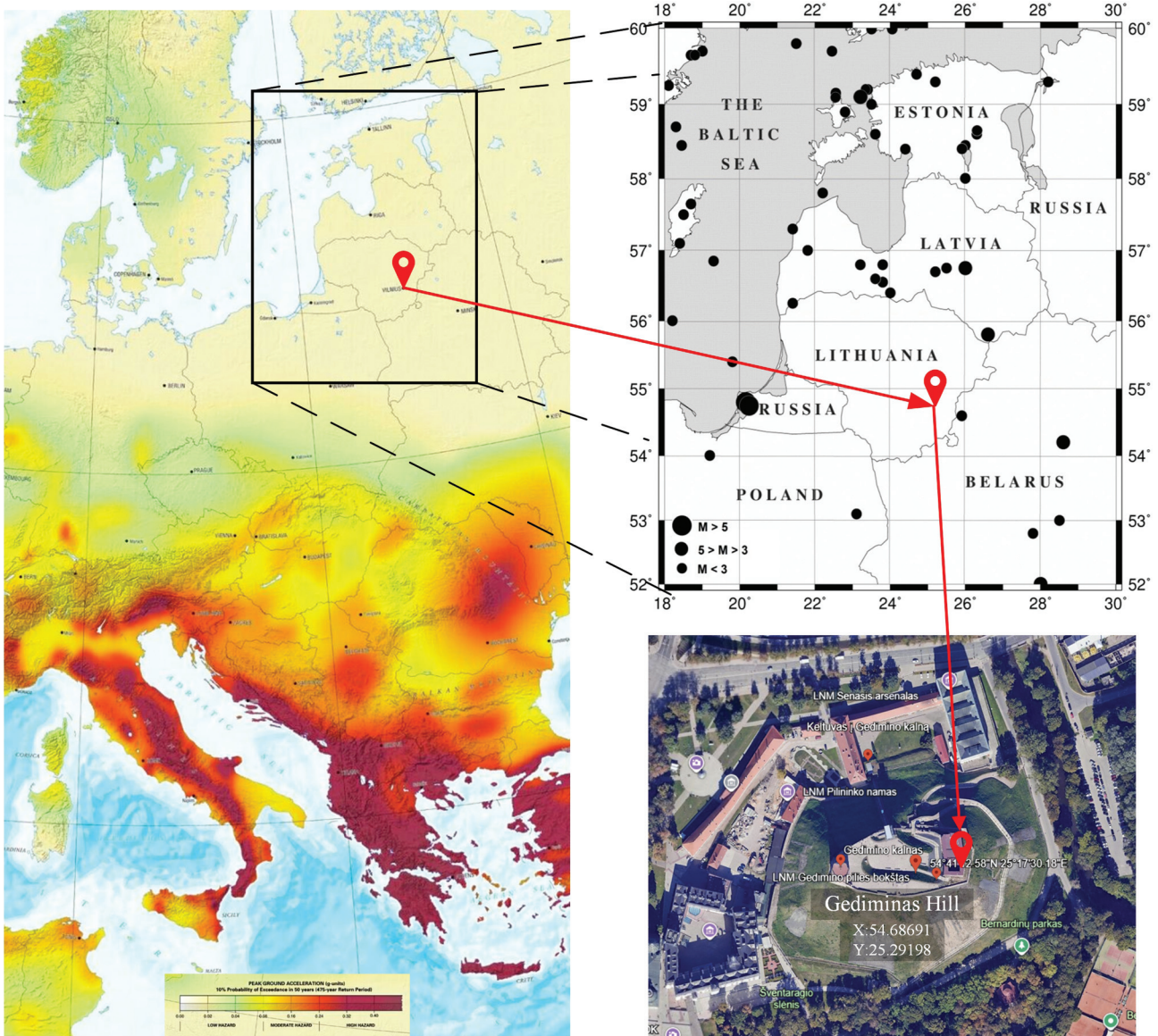


Fig. 1 Location of Gediminas Hill in the map of peak ground acceleration (compiled by M. Zakarka based on Lithuanian Geological Survey (LGT) 2026). Black circles indicate recorded earthquake epicentres; circle size represents approximate magnitude

funicular (Skuodis *et al.* 2017). Fireworks at Gediminas Hill are culturally significant but technically challenging due to dynamic loading and slope instability. Fireworks are often launched nearby during national holidays and city celebrations, making Gediminas Hill a focal point for public gatherings. On Gediminas Hill, the Upper and Lower Castles remains still exist. They are built of brick masonry and have stone walls, brick and stone masonry constructions (Jonaitis *et al.* 2018), lime-based mortars, wooden structures, and in some places reinforced concrete elements, such as retaining walls, foundations and few slabs (Skuodis *et al.* 2023). Gediminas Hill and Upper and Lower Castles remains are of deep national significance for Lithuania as the birthplace of Vilnius, related to the legendary dream of Grand Duke Gediminas and the founding of the capital. Today, the hill and its tower

stand as enduring reminders of Lithuania's medieval heritage and its long struggle for freedom.

Seeking to evaluate Gediminas Hill slope stability, it is necessary to simulate soil and constructions as a huge macro-scale problem with different material types and models in one numerical simulation. The numerical 3D model of Gediminas Hill based on the finite element method (FEM) was prepared using one virtual server of the VILNIUS TECH Information Technology and Systems Centre, with a storage capacity of 1000 GB, 96 CPU cores, and 1536 GB of RAM resources. The generation of the finite element mesh for the numerical model with such IT capacity can take 3–12 hours, while slope stability calculations, depending on the number of modelling stages, may last from 8 hours to several weeks. The first 3D numerical model of Gediminas Hill was a pioneer-

ing FEM simulation created by Skuodis *et al.* (2022). It integrated soils, historic masonry, and modern reinforcements into one macro-scale system, enabling long term slope stability analysis and guiding preservation strategies. This numerical model was continuously improved and supplemented with new information (Skuodis *et al.* 2025). This made it possible to carry out increasingly accurate and detailed numerical calculations, which are calibrated according to monitoring data (Guilhot *et al.* 2021).

Various activities take place on Gediminas Hill; people often gather, celebrate national holidays, and hold concerts. Therefore, various effects occur. For example, shooting fireworks create a dynamic effect. So, the aim of this article is to investigate the impact of fireworks loading on the stability of the slopes of Gediminas Hill, also considering the load from existing constructions. Based on a systematic review on slope stability (Boruah *et al.* 2024), robust models must be developed for a better dynamic load effect evaluation. The objective is to identify potential landslide formation areas, the cause of which could be the dynamic fireworks load on the Upper Castle courtyard of Gediminas Hill.

MODEL AND ENVIRONMENTAL AND FIREWORKS CONDITIONS EVALUATION

The three-dimensional numerical model (See Fig. 2) is created with three-dimensional finite elements by the modelling program DIANA (Diana FEA 2025). The development of the model has been extensively described in previous publications. The program chosen is very convenient for modelling this type problem, as the program contains many different material models and also has very well-developed staged calculations. Material models are critical in the soil–structure interaction because they define how soil and structural components behave under loads. In DIANA FEA, we can choose from several constitutive models depending on the complexity and accuracy required. Soil is nonlinear, anisotropic, and often stress-dependent. For example, the most common Mohr–Coulomb model was used in this model. The main Mohr–Coulomb parameters include cohesion, friction angle, dilatancy angle, elastic modulus, and Poisson’s ratio. This model’s benefit is perfect plasticity after yield, and its general advantages are that it is simple and widely used.

The first goal of the previous modelling (Skuodis *et al.* 2022) was to perform strength reduction analysis and to identify potential landslide locations. Strength reduction analysis (also called the “shear strength reduction method”) is essential for evaluating slope stability in soil mechanics. The purpose of this analysis is to determine the factor of safety (FoS) against slope

failure. Instead of assuming a failure surface (as in limit equilibrium methods), it uses the finite element method (FEM) to find when the slope becomes unstable. In this analysis, soil strength parameters (cohesion and friction angle) are gradually reduced by a factor (Strength Reduction Factor). The FEM model is solved repeatedly until non-convergence occurs (indicating failure). The value of Strength Reduction Factor at failure \approx FoS. It is very needed because FEA predicts a more realistic failure mechanism: FEM captures stress redistribution and deformation patterns. It is good for complex geometries: works for irregular slopes, layered soils, and structures. Therefore, it is better than limit equilibrium. There is no need to pre-define slip surface. The strength reduction in the first model was performed after self-weight and additional load were applied before strength reduction analysis.

Additional calculation was performed by the evaluation of the dynamic force effect. Dynamic load application in soil–structure interaction (SSI) analysis is essential for simulating earthquake effects, machine vibrations, or impact loads high-intensity forces. Such impact load is a short-duration load. Therefore, damping in soil is necessary because real soils dissipate energy during dynamic loading, and this must be represented in the model for realistic results. When waves or vibrations travel through soil, part of energy is lost due to material damping (internal friction between soil particles) and radiation damping (energy escaping to infinity as waves propagate). Without damping, the model would unrealistically amplify vibrations and never reduce oscillations. Also, damping prevents excessive oscillations in time-history analysis and helps achieve convergence in nonlinear dynamic simulations. In this model, Rayleigh damping is evaluated. The mass-proportional parameter controls low-frequency damping. The stiffness-proportional parameter controls high-frequency damping. Typical values of soil damping ratio are 2–5% for sands and 5–10% for clays. Higher damping values are usual for saturated soils or soft clays.

The numerical model of Gediminas Hill soil mass consists of eight main geological layers. The mechanical physical properties of these layers, in the order from the top of the hill, are presented in Table 1. The structures were modelled by evaluating the mechanical properties of elastic material: elastic modulus 2.6 GPa, Poisson’s ratio 0.2, and density 2.9 t/m³. The Mohr–Coulomb constitutive material model was used to evaluate the plasticity of the soils. Since the dynamic effect of the load was evaluated, damping was additionally activated. A consistent damping matrix was evaluated to represent viscous damping.

Dynamic analysis in the soil–structure interaction (SSI) is about simulating how the soil and structure respond to time-dependent loads, such as earthquakes,

Table 1 Physical and mechanical properties of soils

Stratigraphy Index	Youngs modulus [kN/m ²]	Density [t/m ³]	Poisson's ratio	Cohesion [kN/m ²]	Angle of internal friction [°]	Dilatancy angle [°]	Damping ratio	Mass damping parameter	Stiffness damping parameter
tIV-dIV	3600	2.04* and 1.81	0.3	13.5	35.3	0	0.1	0.097	0.092
gdIImd	33100	2.22	0.35	15.3	33.8	3.0	0.1	0.097	0.092
fIImd	56800	1.94	0.3	34.1	38.1	8.0	0.051	0.049	0.047
gdIImd	33100	2.22	0.35	15.3	33.8	3.0	0.1	0.097	0.092
lgIIžm	110700	2.16	0.35	46.2	35.1	5.0	0.047	0.045	0.043
lgIIžm	79200	2.05	0.35	33.0	35.8	6.0	0.05	0.048	0.046
gdIIžm	74200	2.24	0.35	76.9	28.1	2.0	0.1	0.097	0.092
lgIIđn	119900	2.01	0.3	41.7	37.5	7.5	0.1	0.097	0.092

*Saturated density.

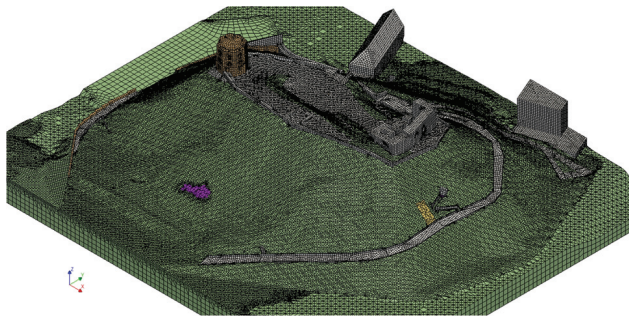


Fig. 2 Gediminas Hill finite element numerical model prepared for static loading and dynamic loading

vibrations, or impacts. Unlike static analysis, the purpose of dynamic analysis is to capture inertia effects (mass and acceleration), to account for damping and wave propagation in soil, and to predict displacements, stresses, and forces during transient events. The governing dynamic equilibrium equation evaluates mass matrix, damping matrix, stiffness matrix, displacement vector, and time-dependent load. For this purpose, transient effects were activated at the analysis tree. The Newmark time integration method was chosen. Dynamic effects and the damping matrix were activated too. Rayleigh damping coefficients a and b were specified in the soil material definitions. The determination of these coefficients followed the formulations presented by Léger and Dussault (1992) and Zerwer *et al.* (2002), in which the principal unknowns are the damping ratio and the characteristic frequencies. After the dynamic load effect was terminated, the strength reduction analysis was initiated.

Compared to other two-dimensional (Duncan, Wright 2014) and three-dimensional (Chen *et al.* 2003; Azizi *et al.* 2020; Su, Shao 2021) slope models, this one is characterized by a large number of different structures and interactions with them.

COMPARISON OF DISPLACEMENTS

Dynamic loads, such as impact loads from fireworks explosions can affect soil displacement on Gediminas Hill in several interconnected ways. Unlike

static loads, dynamic loads vary in magnitude and direction over time. This introduces cyclic stresses into the soil, which can cause stress redistribution within the soil mass. Acceleration forces amplify movement compared to static conditions.

Analysis shows that displacement development is gradual. At the beginning, the initial elastic response is monitored. This means small, reversible movements occur first. Then plastic deformations occur, and with continued loading, permanent displacements develop. Failure can occur if dynamic forces exceed resisting forces, and large-scale slope landslide can develop. Even small cyclic loads can accumulate displacement over time.

The development of landslide depends on soil behaviour under dynamic loading and especially on the reduced shear strength. Repeated loading can lead to a temporary reduction in soil shear strength, especially in saturated soils, due to pore water pressure increase. The consequence of the reduced shear strength was evident when evaluating the strength reduction calculation. Figures 3–7 illustrate the development of displacements during the strength reduction calculation. The evolution of vector displacements is presented for each safety factor for both models in one figure. The figure with label *a* corresponds to the result of the model with the static load. The figure marked *b* corresponds to the result of the model with the dynamic fireworks load. When analyzing these figures, it is important to note that the scales of the results are standardized according to the model without dynamic loading (static). In Figs 3b–6b, the development of displacements is very weak. The displacement zones did not appear because the displacement values correspond to the smallest scale. In a model where dynamic loading is not considered, displacement zones appear from the very beginning. However, in Fig. 7b, a sudden increase in displacement occurs in the model in which the dynamic load was evaluated. Initial estimates of the strength reduction appear to be like the calm before the storm. This has already happened because the effects of dynamic loading have developed landslide zones prior to the strength reduction

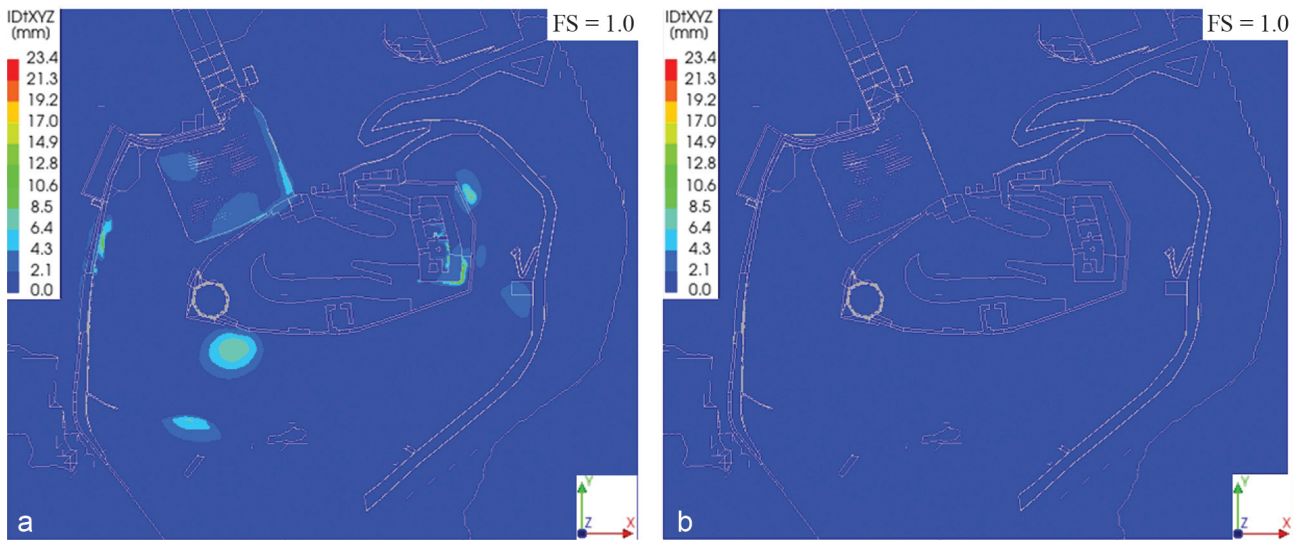


Fig. 3 Development of displacement at strength reduction analysis at factor of safety = 1.0: a) after static loading, b) after dynamic loading

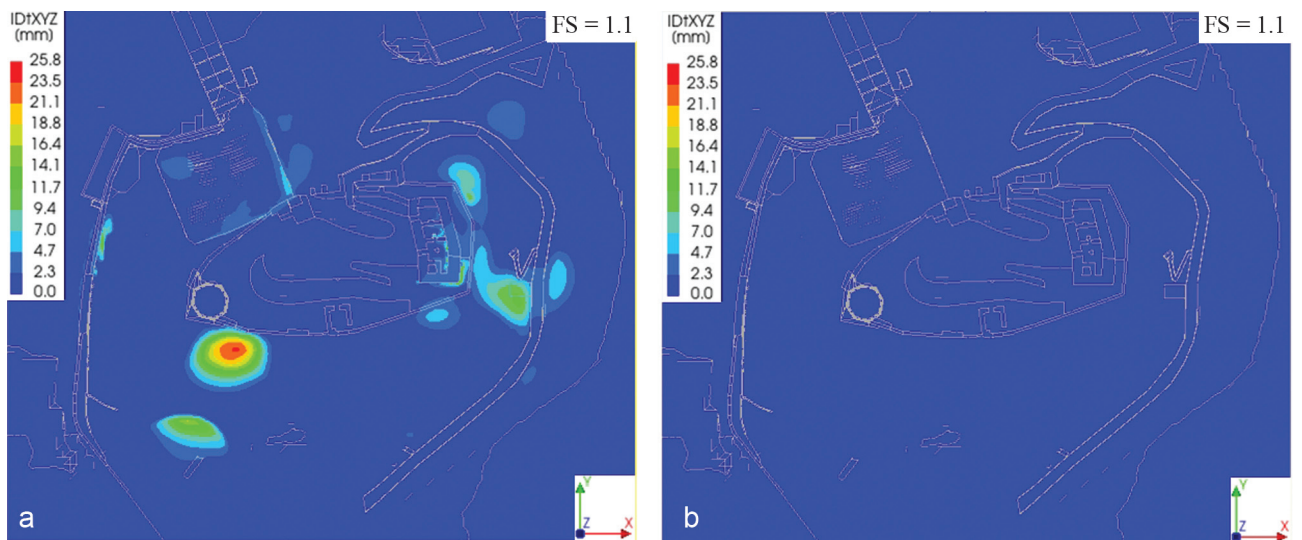


Fig. 4 Development of displacement at strength reduction analysis at factor of safety = 1.1: a) after static loading, b) after dynamic loading

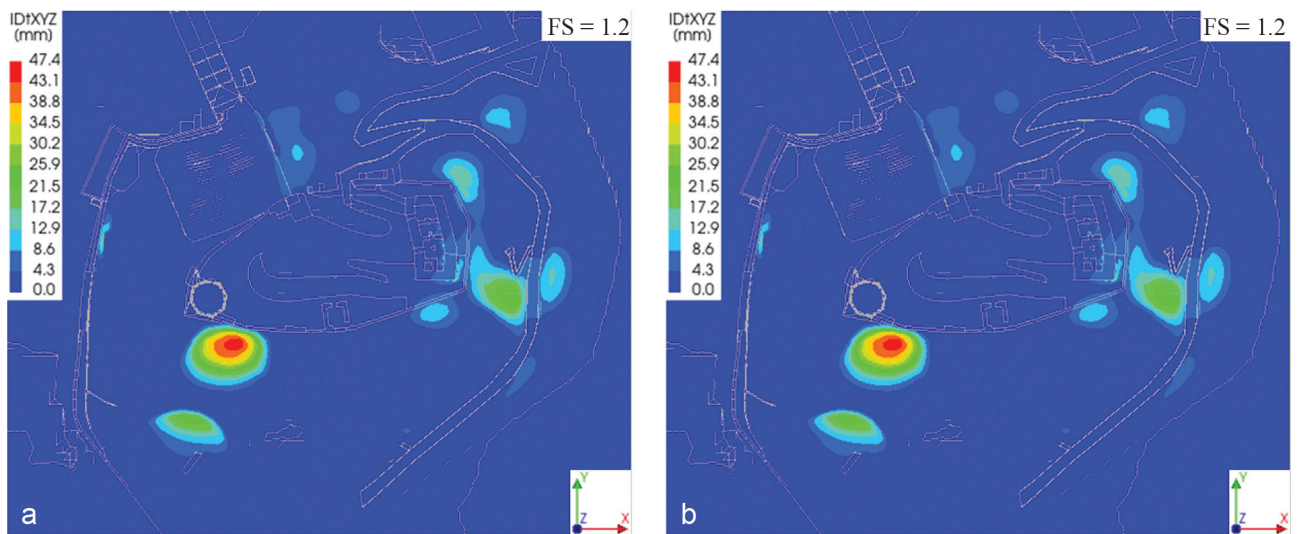


Fig. 5 Development of displacement at strength reduction analysis at factor of safety = 1.2: a) after static loading, b) after dynamic loading

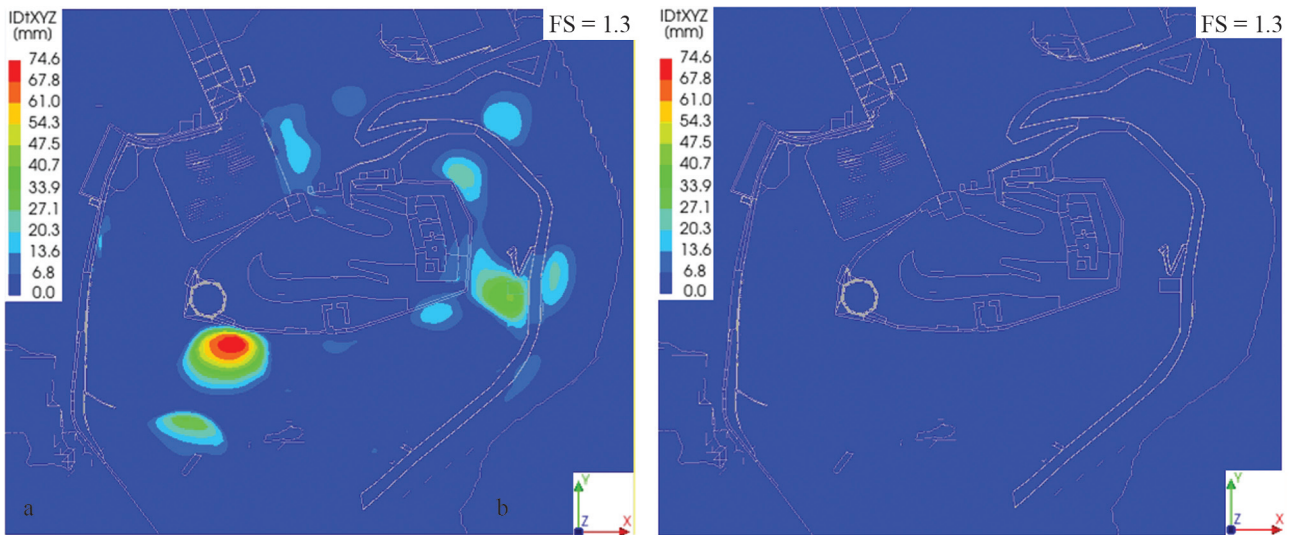


Fig. 6 Development of displacement at strength reduction analysis at factor of safety = 1.3: a) after static loading, b) after dynamic loading

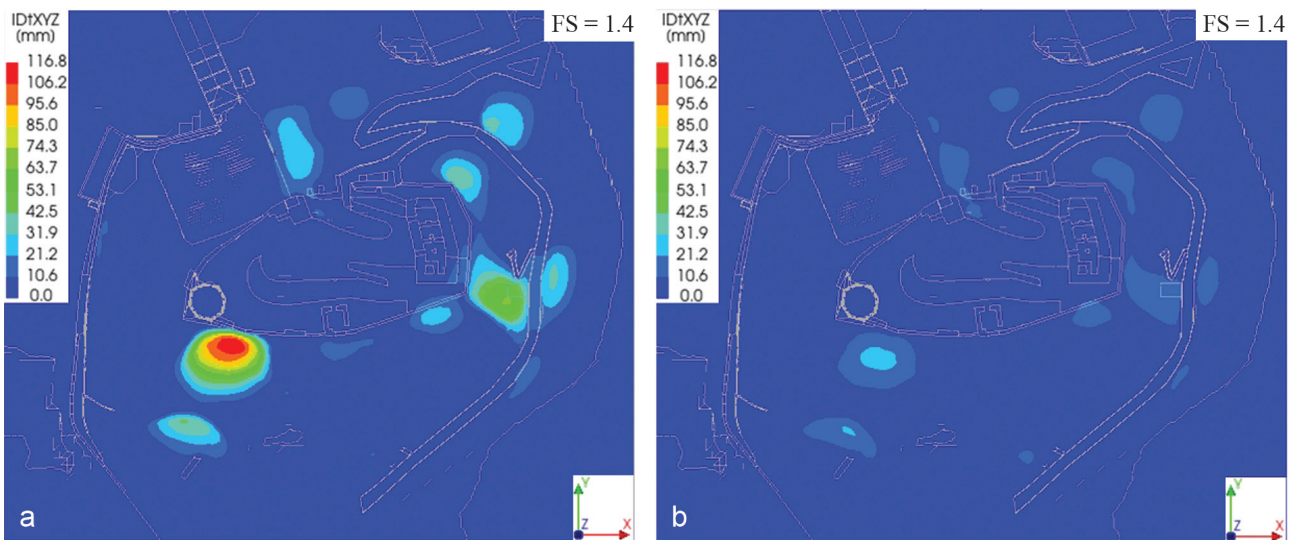


Fig. 7 Development of displacement at strength reduction analysis at factor of safety = 1.4: a) after static loading, b) after dynamic loading

calculation. Therefore, in the initial strength reduction calculations, reducing the cohesion and internal friction angle did not result in significant displacement development. As the strength reduction calculations continue up to a factor of safety of 1.4, displacement increases more rapidly, but not as rapidly as in the model without dynamic loading (see Figs 6–7).

It should be noted that the initiation and formation of the landslide surface becomes clearly identifiable in the numerical model at factors of safety up to approximately 1.3. For higher reduction levels, the numerical simulation represents the post-failure behaviour of the already formed landslide mass rather than the progressive development of a new failure surface. Therefore, displacement results for factors of safety higher than 1.4 are not presented, as they do not provide additional insight into the landslide initiation mechanism.

After reviewing the development of displacements on the surface, it is also necessary to review their development inside the Gediminas Hill, in its layers. The selected section (Fig. 8) is directed through the zone of the greatest displacements at the western tower and runs along the ridge to the Palace of Grand Dukes. This section is important because the landslide with maximum displacements is developing near the tower, and the tower may now potentially lose its integrity and may also lose its stability. Representing displacements in a section allows us to see a more accurate view of the landslide size by estimating the depth at which the displacement develops. The distribution of maximum displacements at the bottom of the layer indicates the initiation of a landslide surface. Figures 9–10 demonstrate the development of vector displacement in depth for factors of safety 1.0 and 1.4. As in the plan view, the development of

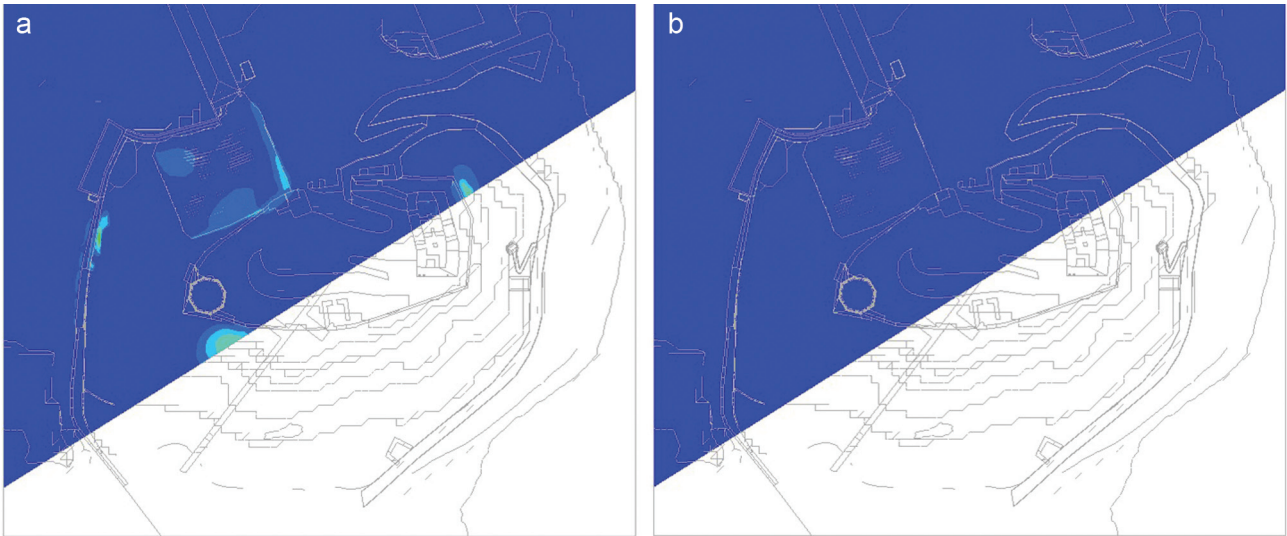


Fig. 8 Section 1-1 position in the plan; a) after static loading, b) after dynamic loading

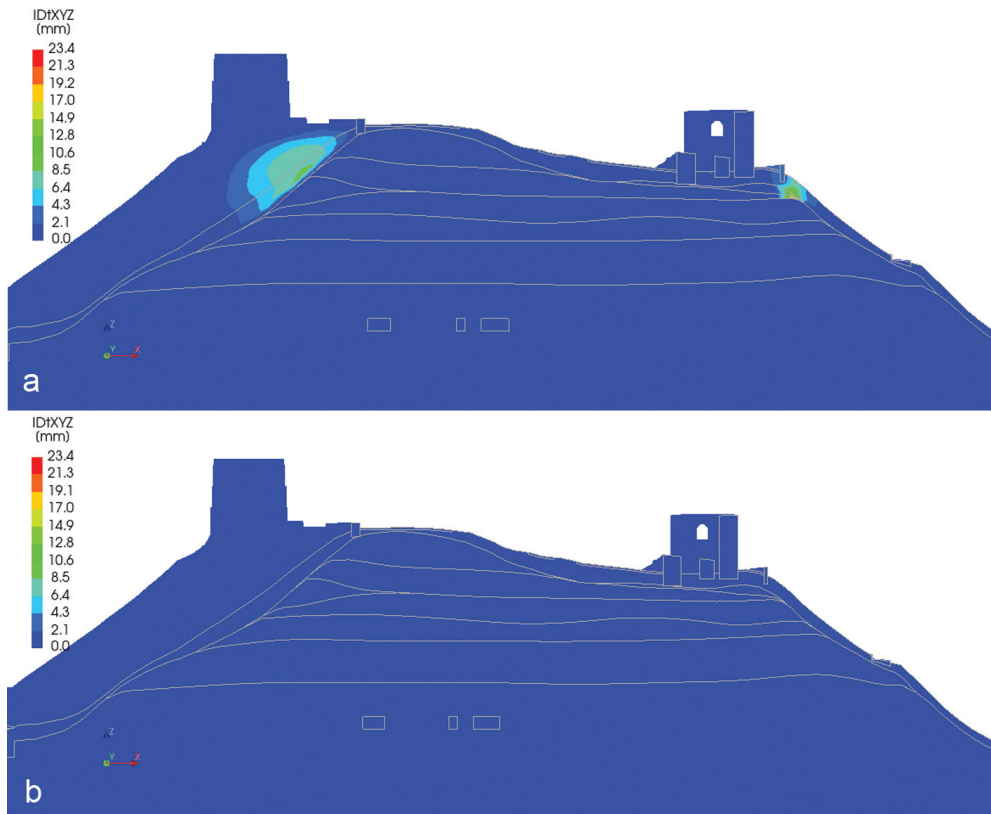


Fig. 9 Development of displacement in section 1-1 at strength reduction analysis at factor of safety = 1.0: a) after static loading, b) after dynamic loading

displacements in the section after the application of dynamic loading remains limited until the factor of safety reaches approximately 1.3. In the model where the load is assessed statically, the maximum displacements tend to develop at the bottom of the technogenic layer (see Fig. 9a). In contrast, in the model where dynamic loading is applied, the maximum displacements are concentrated within the middle part of the technogenic layer already at FoS = 1.4 (see Fig. 10b). For higher strength reduction levels (FoS > 1.4), the

numerical simulation represents the behaviour of the already formed landslide mass rather than the progressive development of a new failure surface; therefore, displacement results for higher factors of safety are not presented. The observed displacement patterns confirm that dynamic loads can trigger shallow landslides or deeper rotational failures when the slope is close to its critical stability.

Another important section 2-2 runs from the western to the eastern slope of the hill (Fig. 11). This sec-

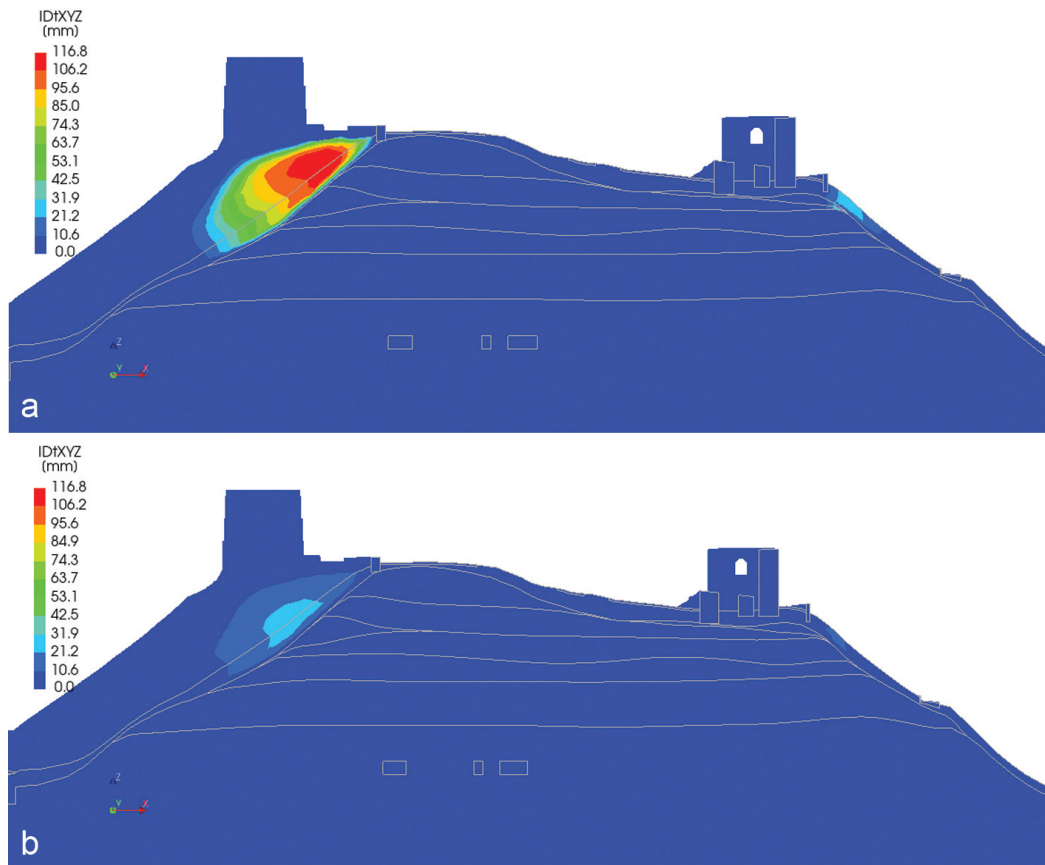


Fig. 10 Development of displacement in section 1-1 at strength reduction analysis at factor of safety = 1.4: a) after static loading, b) after dynamic loading

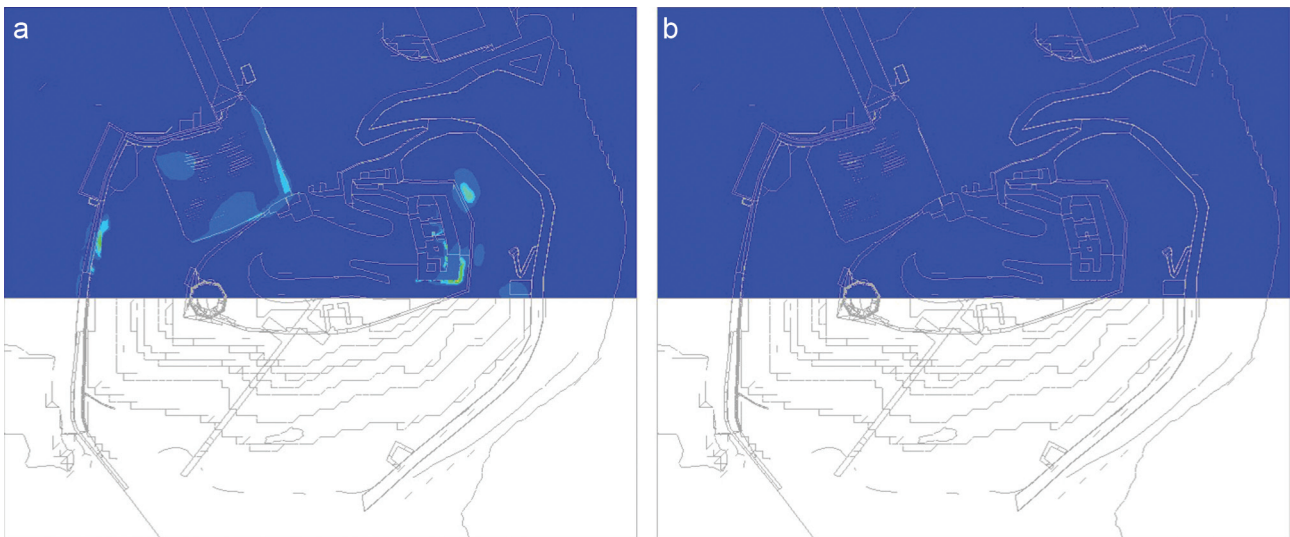


Fig. 11 Section 2-2 position in the plan: a) after static loading, b) after dynamic loading

tion is important because it crosses the western tower on the western slope and the eastern slope at the spring, where landslides have recently occurred. The eastern slope is important because it has the remains of the Palace of Grand Dukes on top and a pedestrian path running below. This slope is under considerable pressure from the remains of the palace, and its stability is particularly important. It is also planned to rebuild the palace here, so the pressure will only in-

crease. But now we only have a picture of the current situation. The development of the vector displacement during the strength reduction calculation in section 2-2 is presented in Figs 12–13. In these Figures, the displacement scale is adjusted according to the maximum displacement results of the model with the static load. In the model with the static load, again the displacement develops from the very first value of the safety factor (see Fig. 12a). In the model where

the dynamic load was evaluated, as the safety factor changes from 1.0 to 1.3, the displacement development is again very small and the displacement zones do not become apparent. Meanwhile, in the model with the static load, displacement develops along the

entire length of the slope; even the remains of the Palace of Grand Dukes sway. The maximum displacement values are distributed almost throughout the entire thickness of the technogenic layer. This indicates that the slip surface is forming over a very large area

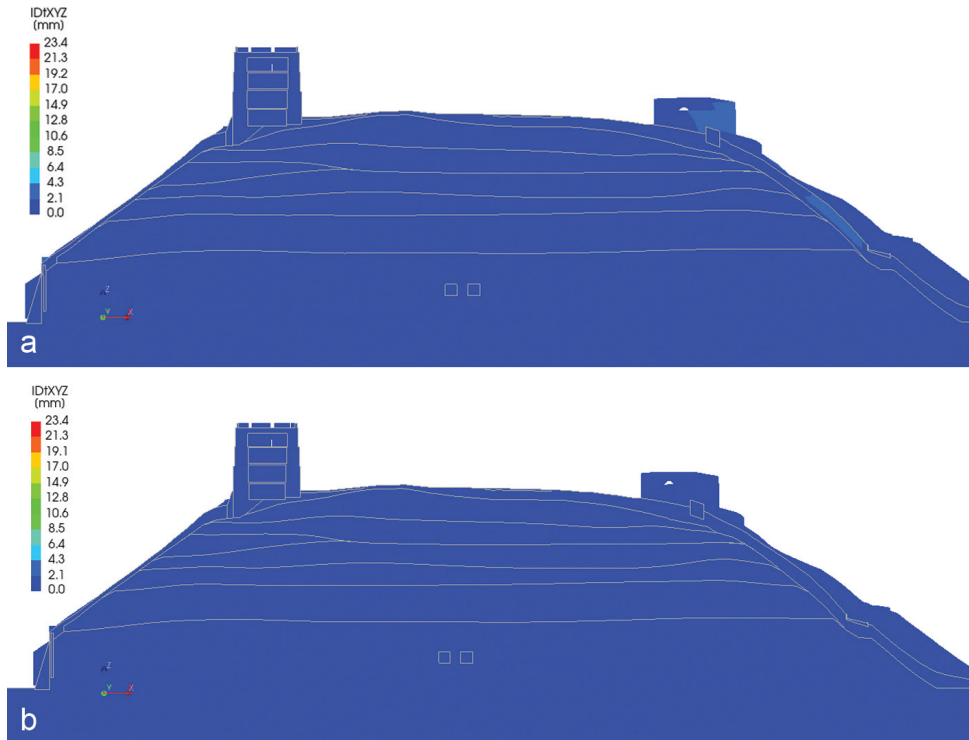


Fig. 12 Development of displacement in section 2-2 at strength reduction analysis at factor of safety = 1.0: a) after static loading, b) after dynamic loading

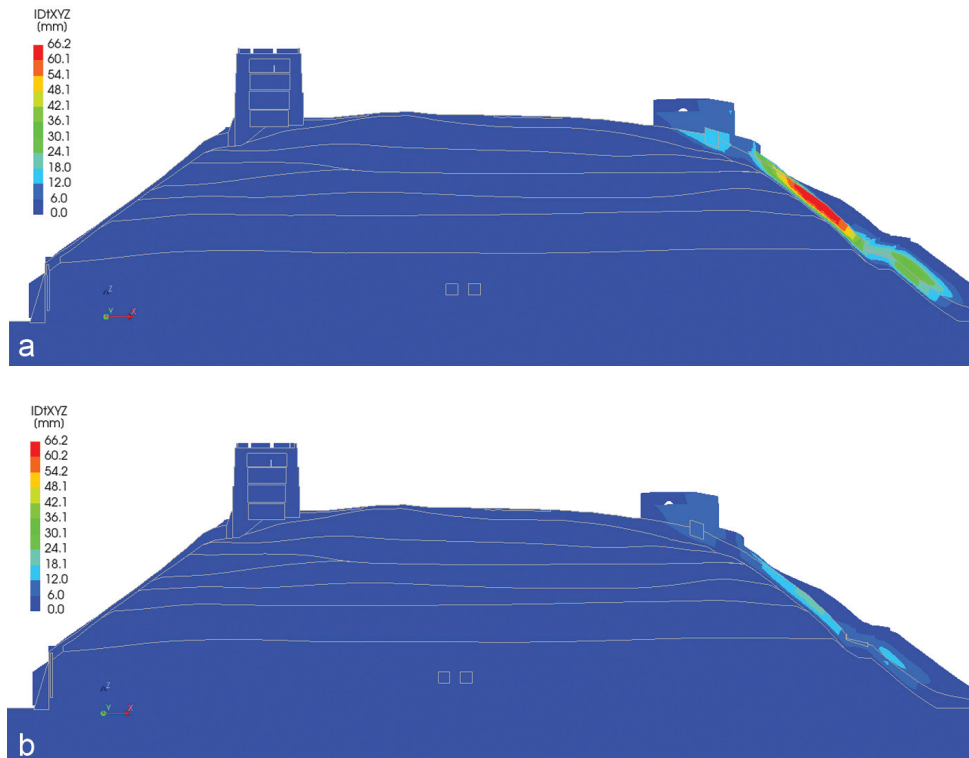


Fig. 13 Development of displacement in section 2-2 at strength reduction analysis at factor of safety = 1.4: a) after static loading, b) after dynamic loading

and even across the entire layer. The displacements of the model with dynamic loading accelerate when the safety factor reaches a value of 1.4 (see Fig.13b). As the safety factor values increase to more than 1.4, the displacement values increase significantly. However, the maximum displacement is distributed at a shallow depth compared to the displacements in the model with static loading. This indicates that slip surfaces form at a shallow depth in the technogenic layer. As the value of the safety factor increases, the maximum displacement occurs at increasingly greater depths. This shows that the sliding surface is constantly changing; initially the size of the sliding surface is small and only at higher values of the safety factor does it increase to the level as in the model with the static load. This explains why the safety factor is higher in the model with dynamic loading. But this does not mean that the effect of dynamic loading increases stability. The danger remains because the increase in displacement after dynamic loading is unnoticeable and sudden. In the static load model, the slip surface initially forms deep in the layer. It is larger than in the model with the dynamic load. Therefore, the safety factor is lower.

The dynamic load assessment showed a different pattern of vector displacement development on slopes during strength reduction analysis. The effect of dynamic loading delayed the development of displacement, while in the model with static loading, the development of displacement is early. The soil compacts due to dynamic effects, but this does not mean that the risk of landslides disappears, since the concentrated mass still moves down the slope.

The peak ground acceleration map (Seismic Hazard Map 2025) shows that for Vilnius city the acceleration value is approximately 0.0059 m/s^2 . The results of numerical simulations showed that on the northeast slope the acceleration value is approximately 0.00574 m/s^2 . Such acceleration was achieved near the remains of the Upper Castle, in other places it is lower.

CONCLUSIONS

The developed numerical model of Gediminas Hill can be used to identify various hazards by assessing various variable factors. This time, the dynamic effect of fireworks was evaluated in the inner square of the hill. Comparisons of the strength reduction results with a model that only evaluated the existing static load are presented. When evaluating the comparisons of the results obtained, we present key observations.

1. The development of a landslide on a map does not show all the important information for assessing the landslide hazard. In the map, we can see the superficial size of the zone. Therefore, it is necessary to

look at the distribution of displacements in the section and identify the slip surface.

2. In the model, after the effect of dynamic loading, during the strength reduction calculation, the maximum displacements are distributed shallowly. The landslide depth correlates with physical and mechanical properties of soil layers. The weakest soil layer is at the Gediminas Hill surface (technogenic soil). Here, the sliding surface is small, but it began to increase sharply and rapidly at high safety factor values. Therefore, it is necessary to respond more seriously to the shifts recorded by the monitoring system. Landslides may develop at shallow depths due to the heterogeneous composition and variable thickness of the technogenic soil layer.

3. Landslide development after static load assessment begins at minimum values of safety factors. The maximum displacements are distributed at greater depths in the layer and the slip surface is larger from the beginning. Therefore, the maximum safety factor was lower in this model.

ACKNOWLEDGMENTS

The authors thank the anonymous reviewers for their constructive comments, which helped to improve the manuscript. This research work has received funding from the project “Civil Engineering Research Centre” (agreement No S-A-UEI-23-5, MSM).

Conflict of interests. The authors declare no conflict of interest. Artificial intelligence (AI) tools were used only for language editing and did not contribute to the scientific content.

REFERENCES

- Azizi, M.A., Marwanza, I., Ghifari, M.K., Anugraha-di, A. 2020. Three dimensional slope stability analysis of open pit mine. In: *Slope Engineering*. IntechOpen. <http://dx.doi.org/10.5772/intechopen.94088>
- Boruah, P.P., Taipodia, J., Chakraborty, A., Anshu, A.K. 2024. A Systematic Review on Slope Stability and Deformation Analysis Subjected to Rainfall and Earthquake. *The Geotechnical Engineering Journal of the SEAGS & AGSSEA* 55(2), 38–52. <https://doi.org/10.14456/seagj.2024.14>
- Chen, Z., Mi, H., Zhang, F., Wang, X. 2003. A simplified method for 3D slope stability analysis. *Canadian Geotechnical Journal* 40(3), 675–683. <https://doi.org/10.1139/t03-002>
- Duncan, J.M., Wright, S.G. 2014. *Soil Strength and Slope Stability*. Hoboken, New Jersey: John Wiley & Sons, Inc.
- Guilhot, D., Martinez Del Hoyo, T., Bartoli, A., Ramakrishnan, P., Leemans, G., Houtepen, M., Salzer, J., Metzger, J.S., Maknavicius, G. 2021. Internet-of-Things-Based Geotechnical Monitoring Boosted by

- Satellite InSAR Data. *Remote Sensing* 13(14), 2757. <https://doi.org/10.3390/rs13142757>
- Jonaitis, B., Antonovič, V., Šneideris, A., Boris, R., Zavalis, R. 2018. Analysis of Physical and Mechanical Properties of the Mortar in the Historic Retaining Wall of the Gediminas Castle Hill (Vilnius, Lithuania). *Materials* 12(1), 8. <https://doi.org/10.3390/ma12010008>
- Lazauskienė, J., Pačesa, A., Satkūnas, J. 2012. Seismotectonic and seismic hazard maps of Lithuania – recent implications of intracratonic seismicity in the Eastern Baltic Region. *Geologija* 54(1), 1–9. <https://doi.org/10.6001/geologija.v54i1.2364>
- Léger, P., Dussault, S. 1992. Seismic-Energy Dissipation in MDOF Structures. *Journal of Structural Engineering* 118(5), 1251–1269. [https://doi.org/10.1061/\(ASCE\)0733-9445\(1992\)118:5\(1251\)](https://doi.org/10.1061/(ASCE)0733-9445(1992)118:5(1251))
- Pagani, M., García-Pelaez, J., Gee, R., Johnson, K., Poggi, V., Simionato, M., Styron, R., Viganò, D., Danciu, L., Monelli, D., Weatherill, G. 2018. *GEM Global Seismic Hazard Map 2018(1)*, 226–251. <https://doi.org/10.13117/GEM-GLOBAL-SEISMIC-HAZARD-MAP-2018.1>
- Skuodis, Š., Kelevišius, K., Žaržojus, G. 2017. Vibrations Measurement of the Funicular Generated Vibrations on Gediminas Hill North Part Slope. In: *Proceedings of 10th International Conference 'Environmental Engineering'*. *Environmental Engineering*. Vilnius Gediminas Technical University, Lithuania: VGTU Technika. <https://doi.org/10.3846/enviro.2017.120>
- Skuodis, Š., Daugevičius, M., Medzvieckas, J., Šneideris, A., Jokūbaitis, A., Rastenis, J., Valivonis, J. 2022. Gediminas Hill Slopes Behavior in 3D Finite Element Model. *Buildings* 12(8), 1113. <https://doi.org/10.3390/buildings12081113>
- Skuodis, Š., Daugevičius, M., Medzvieckas, J., Šneideris, A., Jokūbaitis, A., Rastenis, J., Valivonis, J. 2023. Remains of Gediminas Castle Hill (Vilnius, Lithuania): 3D Numerical Model Behaviour. In: *Modern Building Materials, Structures and Techniques*. Springer. https://doi.org/10.1007/978-3-031-44603-0_1
- Skuodis, Š., Daugevičius, M., Medzvieckas, J., Šneideris, A., Jokūbaitis, A., Rastenis, J., Valivonis, J. 2025. Tunnels in Gediminas Hill (Vilnius, Lithuania): Evaluation of a New Tunnel Found in 2019. *Buildings* 15(14), 2383. <https://doi.org/10.3390/buildings15142383>
- Su, Z., Shao, L. 2021. A three-dimensional slope stability analysis method based on finite element method stress analysis. *Engineering Geology* 280, 105910. <https://doi.org/10.1016/j.enggeo.2020.105910>
- Zerwer, A., Cascante, G., Hutchinson, J. 2002. Parameter Estimation in Finite Element Simulations of Rayleigh Waves. *Journal of Geotechnical and Geoenvironmental Engineering* 128(3), 250–261. [https://doi.org/10.1061/\(ASCE\)1090-0241\(2002\)128:3\(250\)](https://doi.org/10.1061/(ASCE)1090-0241(2002)128:3(250))

Internet sources

- EFEHR Risk Maps. <https://maps.eu-risk.eucentre.it/> [Accessed November 2025].
- Lithuanian Geological Survey (LGT). <https://lgt.lrv.lt/lt/apie-lietuvos-zemes-gelmes/seismologija/bendra-informacija/> [Accessed November 2025].
- Diana FEA. 2025. DIANA Finite Element Analysis User's Manual, Release 10.1. DIANA FEA BV. <https://Manuals.Dianafea.Com/D101/Analys/Node578.Html> [Accessed November 2025].